UNIVERSIDADE DE SÃO PAULO

INSTITUTO DE FÍSICA
CAIXA POSTAL 66318
05315-970 SÃO PAULO - SP
BRASIL

PUBLICAÇÕES

IFUSP/P-1286

VARIANCES AND COVARIANCES IN DECONVOLUTION OF MULTICHANNEL SPECTRA

O. Helene and **C. Takiya**
Instituto de Física, Universidade de São Paulo

Outubro/1997

Pág. 1 - 12

Variances and covariances in deconvolution of multichannel spectra

O. Helene and C. Takiya

Instituto de Física, Universidade de São Paulo

CP 66318 CEP 05315-970 São Paulo, SP, Brazil.

Abstract

This paper discusses some aspects of deconvolution of one-dimensional spectra in the framework of the Least Squares Method. Covariance matrices are taken into account in every step. Fluctuation and artifacts, both in the deconvolved and regularized spectra, can be interpreted from the structure of the covariance matrices. The method is applied to a simulated spectrum.

I. INTRODUCTION

Deconvolution of one dimensional spectra has been extensively used in experimental sciences in connection to gamma-ray spectroscopy [1], neutron [2,3], mass [4], and beta [5] spectra study, cross-section measurements [7], energy distribution of annihilation radiation [6,8], microprobe scans [9], among others. The basic goal of deconvolution procedures is to obtain the intrinsic distribution of a signal blurred by the response function of a detector system and affected by statistical fluctuation. The main source of troubles in deconvolution algorithms is that even small statistical fluctuations in the original data are strongly amplified [10] and, frequently, produce an oscillatory behavior of the data, and negative counts. In order to reduce fluctuations of the deconvolved spectra many regularization procedures have been developed [11]. Usually, such regularization procedures have been studied from ad hoc observations of the obtained results in some practical and simulated cases. However, regularization methods give rise to biased estimates and artifacts, and the choice of the regularization parameter depends on the compromise between the bias of the estimate and its noise component [12].

In the study of deconvolution procedure, not enough attempt has been paid to the covariance matrices. As pointed out in this paper, information obtained from the structure of the covariance matrices can be useful in understanding the behavior of deconvolved spectra: the large fluctuations are related to the large elements on the diagonal of the covariance matrices; and the oscillatory behavior of the deconvolved spectrum is consequence of the negative elements on both sides of the main diagonal of the covariance matrices. This paper discusses some aspects of the deconvolution procedure within the Least Squares Method (LSM), and takes into account, in every step, the covariance matrices. If the covariance matrices are taken into account, the obtained results are unbiased, the artifacts can be understood, functions can be fitted to the data, and the goodness-of-fit can be tested by the usual chi-square test.

II. LEAST SQUARES METHOD AND REGULARIZATION PROCEDURES

The relationship between an unknown spectrum $S(x')$ and the measured spectrum Y_i can be described by

$$Y_i = \int R_i(x')S(x')dx' + \epsilon_i, \tag{1}$$

where $R_i(x')$ is the detector response function, and ϵ_i is a measurement error. Eq.(1) can be expressed approximately as

$$Y_i = \sum_j R_{ij}S(x_j) + \epsilon_i \tag{2}$$

where

$$R_{ij} = \int_{x_j-\frac{1}{2}}^{x_j+\frac{1}{2}} R_i(x')dx' \tag{3}$$

Eq. (2) can be written in a more suitable form as

$$\mathbf{Y} = \mathbf{R}\cdot\mathbf{S} + \vec{\epsilon} \tag{4}$$

where $\mathbf{Y}$ is the known column vector with elements Y_i, $\mathbf{R}$ is the response matrix, $\mathbf{S}$ the unknown (column) vector with elements $S(x_i)$ and $\vec{\epsilon}$ is the error vector. Although $\vec{\epsilon}$ is unknown we have $< \vec{\epsilon} >= 0$ and $< \vec{\epsilon}\cdot\vec{\epsilon}^{\,t} >= \mathbf{V}$, where $\mathbf{V}$ is the covariance matrix of $\mathbf{Y}$, and $<>$ stands for expectation value. Due to the linear relation between the vector of observations, $\mathbf{Y}$, and the vector of parameters, $\mathbf{S}$, the optimum estimate $\tilde{\mathbf{S}}$ is given by the LSM,

$$\tilde{\mathbf{S}} = (\mathbf{R}^t\mathbf{V}^{-1}\mathbf{R})^{-1}\mathbf{R}^t\mathbf{V}^{-1}\mathbf{Y}. \tag{5}$$

$\tilde{\mathbf{S}}$ is consistent, unbiased and the minimum variance estimator of $\mathbf{S}$. No other linear estimator can be better than $\tilde{\mathbf{S}}$ [13]. The covariance matrix of $\tilde{\mathbf{S}}$ is given by

$$\mathbf{V}_{\tilde{\mathbf{S}}} = (\mathbf{R}^t\mathbf{V}^{-1}\mathbf{R})^{-1} \tag{6}$$

Eqs. 5 and 6 can be fruitfully used both in the deconvolution procedure, and in the interpretation of the deconvolved spectra, both related to the large fluctuation of the results, and the source artifacts.

Regularization procedures can be put into the above framework. For instance, smoothing procedures can be represented by the multiplication of $\tilde{\mathbf{S}}$ by some suitable matrix. In this case, the regularized spectrum is given by

$$\mathbf{S_T} = \mathbf{T}\cdot\tilde{\mathbf{S}}, \tag{7}$$

and the covariance matrix of $\mathbf{S_T}$ given by

$$\mathbf{V_T} = \mathbf{T}\cdot\mathbf{V_S}\cdot\mathbf{T^t}. \tag{8}$$

Eqs. 7 and 8 must be used in order to understand both the reduction of the very large fluctuations of $\tilde{\mathbf{S}}$, and the source of artifacts.

III. SIMULATION

The convolution of two Gaussians is a Gaussian with variance equal to the sum of the variances of the partial Gaussians. Thus, the deconvolution of a Gaussian peak using as response function a Gaussian, results in a Gaussian peak. So, in order to study some practical aspects of the deconvolution procedure using the LSM and taking into account the covariance matrices, a spectrum containing a Gaussian peak with a standard deviation of 5.00 channels and an area of 100,000 counts, superimposed to an uniform background of 200 counts per channel was simulated. A Poisson random fluctuation was added to every channel in order to simulate the typical statistical fluctuation of real spectra. Fig 1 shows the simulated peak. Results of the fitting of a Gaussian peak are shown in Table I.

A. Deconvolution

The simulated peak was deconvolved using eq. 5 with

$$R_{ij} = \int_{j-\frac{1}{2}}^{j+\frac{1}{2}} \int_{i-\frac{1}{2}}^{i+\frac{1}{2}} \frac{1}{\sqrt{2\pi}\cdot\sigma_r} \cdot e^{-(x_i-x_j)^2/2\sigma_r^2} \cdot dx_i dx_j \qquad (9)$$

with $\sigma_r = 1.2$ channel. Fig. 2 shows the obtained spectrum with enormous fluctuation, typical of deconvolution procedures. The peak structure was apparently lost and non physical (yet statistically necessary) negative counts appear. The structure of the spectrum in fig. 2 can be understood inspecting the covariance matrix calculated from eq.6 (assuming $\mathbf{V}$ a diagonal matrix with $V_{ii} = Y_i$). Table II shows the central part of $\mathbf{V_{\tilde{S}}}$. The variances of $\tilde{S}$ are about 10^9, corresponding to standard deviation of about $3 \cdot 10^4$, greater than the typical values of $\mathbf{Y}$ in the peak region (about 10^4), and many times greater than $\sqrt{Y_i}$. Those standard deviations explain the enormous fluctuations of $\tilde{\mathbf{S}}$. The typical oscillation pattern of $\tilde{\mathbf{S}}$ can also be understood from the inspection of $\mathbf{V_{\tilde{S}}}$ or, better, the correlation between counts in adjacent channels, defined as

$$\rho_{ij} = \frac{(\mathbf{V_{\tilde{S}}})_{ij}}{\sqrt{(\mathbf{V_{\tilde{S}}})_{ii}(\mathbf{V_{\tilde{S}}})_{jj}}}. \qquad (10)$$

As can be seen from Table II, the correlations between counts in adjacent channels are about -0.98. A negative correlation between two data means that if a datum is underestimated (overestimated) the other is probably overestimated (underestimated). As a consequence, the empirical value of the correlation between counts in adjacent channels explain the strong oscillatory shape of the deconvolved spectrum $\tilde{\mathbf{S}}$ of Figure 2.

In spite of the strange pattern of the spectrum in Fig 2, the LSM can be used in order to fit the peak and background. Table I shows the result of the fitting of a Gaussian peak to $\tilde{\mathbf{S}}$, taking into account the covariance matrix of $\tilde{\mathbf{S}}$. The obtained standard deviation, $\sigma = 4.863(14)$, agrees with expected value ($\sqrt{5^2 - 1.2^2} = 4.854$). Likewise, the area, position and background agree with the expected values. The obtained reduced chi-square value, 1.04 with 247 degrees of freedom, corresponds to 32% confidence level and shows that both the fit is acceptable and no more hypothesis are needed to explain the structure of the spectrum.

B. Regularization

Fig. (3) shows the same data regularized by applying $\mathbf{T}$ (Eq. 7) on $\tilde{\mathbf{S}}$ with

$$T = \begin{bmatrix} \frac{1}{4} & \frac{1}{2} & \frac{1}{4} & 0 & 0 & 0 & 0 & \dots \\ 0 & \frac{1}{4} & \frac{1}{2} & \frac{1}{4} & 0 & 0 & 0 & \dots \\ 0 & 0 & \frac{1}{4} & \frac{1}{2} & \frac{1}{4} & 0 & 0 & \dots \\ \vdots & \vdots & \vdots & \dots & \dots & \vdots & \vdots & \vdots \end{bmatrix}. \qquad (11)$$

Table III shows the covariance/correlation matrix of the central part of $\mathbf{S_T} = \mathbf{T} \cdot \tilde{\mathbf{S}}$. As can be seen by comparing the diagonal elements of $\mathbf{V_T}$ (table III) with the diagonal elements of $\mathbf{V_S}$ (table II), variances were reduced by a factor of about 10^3. Such reduction can be understood by inspecting the regularization procedure. If σ_1, σ_2 and σ_3 are the standard deviations of the counts in three adjacent channels and $\rho_{ij} \cdot \sigma_i \cdot \sigma_j$ (j=1,2,3) their covariances, the variance of the number of counts in a regularized channel is

$$\sigma^2_{reg} = \frac{\sigma_1^2}{16} + \frac{\sigma_2^2}{4} + \frac{\sigma_3^2}{16} + \frac{\rho_{12}\cdot\sigma_1\sigma_2}{4} + \frac{\rho_{13}\cdot\sigma_1\sigma_3}{8} + \frac{\rho_{23}\cdot\sigma_2\sigma_3}{4}. \qquad (12)$$

Since $\rho_{12} \cong \rho_{23} \cong -\rho_{13}$, $\rho_{12} \cong -1$ and $\sigma_1 \cong \sigma_2 \cong \sigma_3 \cong \sigma$ we have $\sigma^2_{reg} << \sigma^2$. As a conclusion, it is the strong and negative feature of the covariance between adjacent counts in the deconvolved spectrum that makes the regularization procedures useful. Table I shows the results of fitting a Gaussian peak superimposed to an uniform background to data in figure 3 using the LSM and taking into account the whole covariance matrix of $\mathbf{S_T}$. The reduced χ^2 is 0.9855 with 245 degrees of freedom and corresponds to a 55% confidence level. Small differences between the fitted values of the area, position, and background in the simulated, deconvolved, and regularized spectra in Table 1 are due to the fact that the widths of the peaks in the three spectra are different. (The deconvolved spectra is narrower than the original spectrum, and the regularized spectrum is wider than the deconvolved one due to smoothing).

IV. CONCLUSION

The basic equation of the convolution problem is the discrete case is given by Eq. 4. Due to the linear relation between experimental data, $\mathbf{Y}$, and unknown parameters, $\mathbf{S}$, the best solution is given by the LSM. The LSM gives the minimum variance unbiased estimator of $\mathbf{S}$ and it can be shown [13] that any other linear estimator of $\mathbf{S}$ has variances greater than the variances of $\tilde{\mathbf{S}}$. So, no other method can be better than the LSM. However, deconvolution procedures give rise to covariant data. Thus, in order to preserve the statistical properties of the results, it is necessary to consider the covariance matrix $\mathbf{V}_{\tilde{\mathbf{S}}}$.

If regularization methods are to be employed in order to recover the lost visual profile of the deconvolved spectra, the covariance matrix must be calculated by using Eq. 8. However, as shown in the example, the regularized spectrum do not have more information than the deconvolved spectrum.

By inspecting the covariance matrices we can understand the large fluctuations, the oscillatory pattern, and the artifacts existing in the deconvolved and regularized spectra.

Finally, it must be taken into account that, although regularized spectra are better than the deconvolved spectra under a visual aspects, both usually have artifacts and can induce misinterpretation of the data.

ACKNOWLEDGMENTS

We acknowledge the critical reading of the manuscript by Dr. P. Gouffon. This work was partially supported by CNPq.

REFERENCES

[1] Cs. Süsköd, W. Galster, I. Licot and M. P. Simonart, Nucl. Instr. and Meth. **A355** (1995) 552.

[2] J. Půlpán and M. Králí k, Nucl. Instr. and Meth. **A325** (1993) 314.

[3] W. R. Burrus and V. V. Verbisnki, Nucl. Instr. and Meth. **A67** (1969) 181.

[4] A. A. Marchetti and A. C. Mignerey, Nucl. Instr. and Meth. **A324** (1993) 288.

[5] Thomas M. Semov, Appl. Radiat. Isot. **46** (1995) 341.

[6] J. Dryzek, C. A. Quartes, Nucl. Instr. and Meth. **A378** (1996) 337.

[7] B. C. Cook, Nucl. Instr. and Meth. **24** (1963) 256.

[8] L. Hoffmann, A. Shukla, M. Peter, B. Barbiellini and A. A. Manuel, Nucl. Instr. and Meth. **A335** (1993) 276.

[9] G. E. Coote and Betty P. Kwan, Nucl. Instr. and Meth. **B104** (1995) 228.

[10] Per Christian Hansen, Inverse Problems **8** (1992) 849.

[11] V. B. Anikeev and V. P. Zhigunov, Phys. Part. Nucl. **24** (1993) 424.

[12] V. B. Anikeev A. A. Spiridonov and V. P. Zhigunov, Nucl. Instr. and Meth. **A(303)** (1991) 350.

[13] M. G. Kendall and A. Stuart, "The Advanced Theory of Statistics" (Charles Griffin and Co Ltd., London, 1967), Vol. 2.

TABLES

	Simulated	Deconvolved	Regularized
Area (counts)	100,007(327)	100,305(327)	100,022(327)
Position (channels)	124.978(17)	124.980(17)	124.979(17)
σ (channels)	5.007(14)	4.863(14)	4.896(14)
Background (counts per channel)	198.06(95)	197.95(95)	198.21(96)
Reduced χ^2 P(χ^2)	0.99 (55 %)	1.04(32 %)	0.99 (55 %)

TABLE I. Result of the fit of a Gaussian peak plus a background to the original (second column), the deconvolved (third column), and the regularized spectra (fourth column).

	(121)	(122)	(123)	(124)	(125)	(126)	(127)	(128)	(129)
(121)	0.730E9	-0.768E9	0.772E9	-0.744E9	0.689E9	-0.616E9	0.534E9	-0.450E9	0.371E9
(122)	-0.984	0.834E9	-0.865E9	0.857E9	-0.812E9	0.740E9	-0.651E9	0.556E9	-0.463E9
(123)	0.940	-0.984	0.927E9	-0.947E9	0.923E9	-0.861E9	0.773E9	-0.670E9	0.563E9
(124)	-0.871	0.938	-0.984	0.999E9	-0.101E10	0.966E9	-0.887E9	0.784E9	-0.670E9
(125)	0.789	-0.869	0.937	-0.983	0.105E10	-0.104E10	0.980E9	-0.887E9	0.772E9
(126)	-0.700	0.786	-0.868	0.937	-0.983	0.106E10	-0.104E10	0.965E9	-0.861E9
(127)	0.612	-0.697	0.784	-0.867	0.937	-0.983	0.104E10	-0.100E10	0.922E9
(128)	-0.528	0.609	-0.696	0.784	-0.867	0.937	-0.983	0.999E9	-0.946E9
(129)	0.452	-0.526	0.608	-0.696	0.784	-0.868	0.937	-0.983	0.926E9

TABLE II. Covariance (upper triangle, including the main diagonal) and correlation (lower triangle) matrix of the central part of de deconvolved spectrum by using the LSM method. The numbers into parenthesis refer to the channel number of the spectrum.

	(121)	(122)	(123)	(124)	(125)	(126)	(127)	(128)	(129)
(121)	0.364E6	-0.286E6	0.100E6	0.670E5	-0.155E6	0.171E6	-0.144E6	0.102E6	-0.620E5
(122)	-0.744	0.408E6	-0.315E6	0.108E6	0.719E5	-0.163E6	0.176E6	-0.146E6	0.102E6
(123)	0.249	-0.741	0.443E6	-0.339E6	0.114E6	0.748E5	-0.166E6	0.177E6	-0.144E6
(124)	0.162	0.246	-0.742	0.472E6	-0.351E6	0.115E6	0.757E5	-0.164E6	0.172E6
(125)	-0.373	0.163	0.247	-0.741	0.477E6	-0.349E6	0.112E6	0.728E5	-0.155E6
(126)	0.415	-0.373	0.164	0.244	-0.740	0.468E6	-0.338E6	0.108E6	0.663E5
(127)	-0.359	0.414	-0.374	0.165	0.244	-0.741	0.444E6	-0.317E6	0.101E6
(128)	0.265	-0.358	0.415	-0.373	0.165	0.246	-0.742	0.410E6	-0.289E6
(129)	-0.170	0.265	-0.359	0.414	-0.372	0.160	0.252	-0.746	0.366E6

TABLE III. Covariance (upper triangle, including the main diagonal) and correlation (lower triangle) matrix of the central part of regularized spectrum.

FIGURES

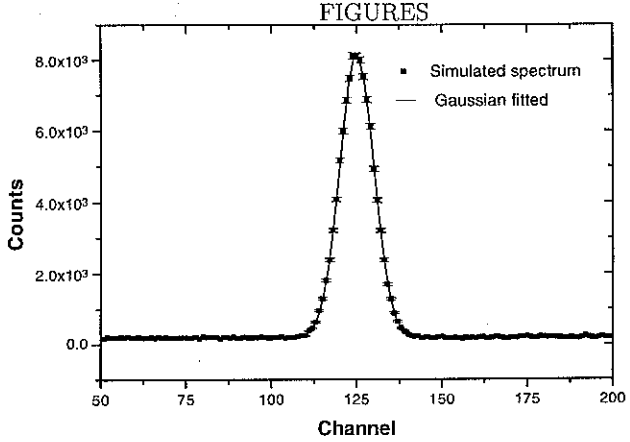

FIG. 1. Simulated spectrum and the fitted peak plus background.

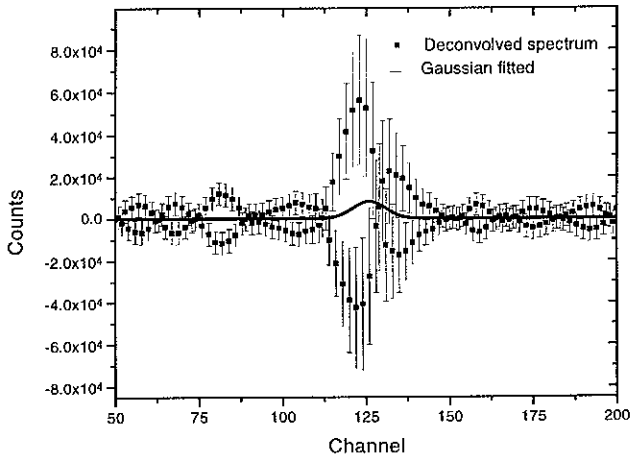

FIG. 2. Deconvolved spectrum by using the LSM method and the fitted peak and background.

FIG. 3. Regularized spectrum and the fitted curve.